Article

The Role of the Peripheral Anionic Site and Cation–π Interactions in the Ligand Penetration of the Human AChE Gorge

Davide Branduardi, Francesco Luigi Gervasio, Andrea Cavalli, Maurizio Recanatini, and Michele Parrinello

J. Am. Chem. Soc., **2005**, 127 (25), 9147-9155• DOI: 10.1021/ja0512780 • Publication Date (Web): 01 June 2005

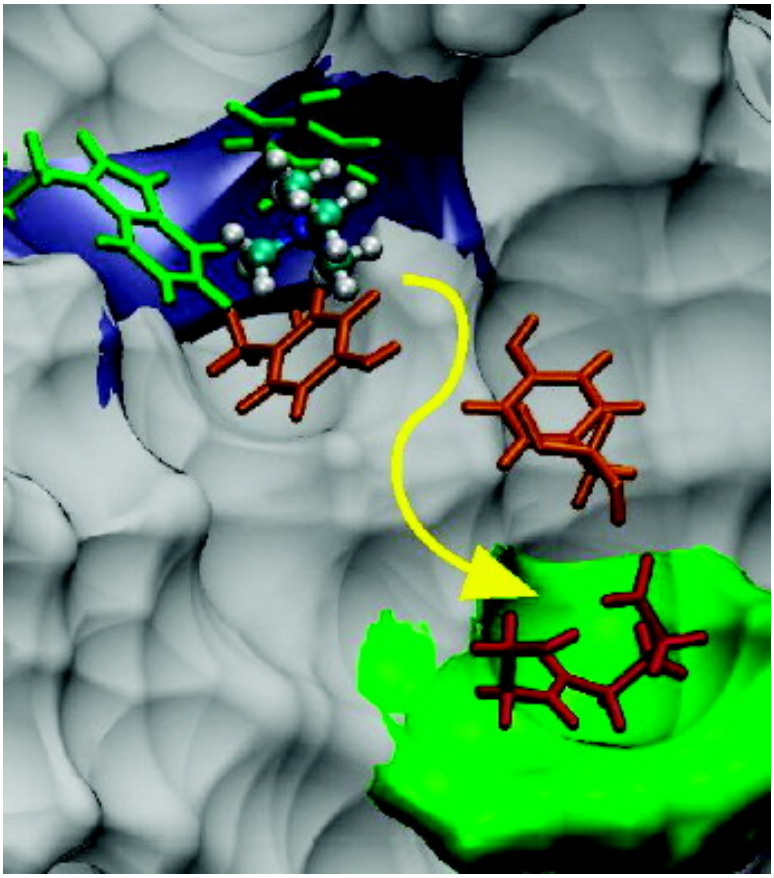

J|A|C|S
ARTICLES
Published on Web 06/01/2005

The Role of the Peripheral Anionic Site and Cation−π Interactions in the Ligand Penetration of the Human AChE Gorge

Davide Branduardi,[†] Francesco Luigi Gervasio,*[,†] Andrea Cavalli,*[,‡] Maurizio Recanatini,[‡] and Michele Parrinello[†]

Contribution from the Computational Sciences, Department of Chemistry and Applied Biosciences, ETH Zürich, USI Campus, Via Giuseppe Buffi 13, CH-6900 Lugano, Switzerland, and Department of Pharmaceutical Sciences, University of Bologna, Via Belmeloro 6, I-40126 Bologna, Italy

Received March 1, 2005; E-mail: fgervasi@phys.chem.ethz.ch; andrea.cavalli@unibo.it

Abstract: We study the ligand (tetramethylammonium) recognition by the peripheral anionic site and its penetration of the human AChE gorge by using atomistic molecular dynamics simulations and our recently developed metadynamics method. The role of both the peripheral anionic site and the formation of cation−π interactions in the ligand entrance are clearly shown. In particular, a simulation with the W286A mutant shows the fundamental role of this residue in anchoring the ligand at the peripheral anionic site of the enzyme and in positioning it prior to the gorge entrance. Once the ligand is properly oriented, the formation of specific and synchronized cation−π interactions with W86, F295, and Y341 enables the gorge penetration. Eventually, the ligand is stabilized in a free energy basin by means of cation−π interactions with W86.

Introduction

Acetylcholinesterase (AChE, EC 3.1.1.7) is a serine hydrolase that plays a key role in terminating the nervous signal, by hydrolyzing the neurotransmitter acetylcholine.[1] For this reason, it is of primary pharmaceutical interest. Its inhibition is one of the most successful strategies in the reinforcement of the cholinergic transmission. In the last two decades, AChE has been the focus of intense pharmaceutical research that culminated in the development of a number of drugs currently in clinical use for the treatment of Alzheimer's disease.[2] Moreover, AChE performs a wide range of noncatalytic functions, spanning from cell adhesion to neuritogenesis and synaptogenesis, and from haematopoiesis and thrombopoiesis to promotion of amyloid-β (Aβ) fibrillization.[3] The latter activity, demonstrated in vitro and in vivo by several teams of researchers,[4−6] is particularly intriguing because it can be related to the neuropathological cascade leading to Alzheimer's-type dementia.[7] Independent studies carried out by different laboratories led to the conclusion that the site responsible for the noncatalytic actions coincides or is very close to the so-called peripheral anionic site (PAS) of the enzyme. This site consists of a pool of amino acids located around the key residue W286.[8,9] These evidences led to a renewed interest in the search for AChE inhibitors capable of binding not only to the catalytic site but also to the AChE PAS, and thus possibly preventing the chaperon-like action of AChE toward the Aβ fibrillization.[10,11]

The role of the AChE PAS in quaternary cationic ligand recognition has been widely discussed in the literature.[12] After an initial phase when the protein electric field attracts the ligand,[13,14] atomistic interactions with the PAS come into play. This is supported by a study of Shafferman and co-workers, in which a key residue of the PAS, namely, the W286 (see Figure 1), was mutated into A. The mutant showed modified kinetics.[15] Recent X-ray experiments[16] confirmed this central role of W286 in binding cationic ligands. However, the passage from the PAS to the internal gorge of the AChE has to be further clarified, making it an ideal candidate for an in-depth computational study. Indeed, the availability of high-resolution X-ray structures of the enzyme alone or co-crystallized with various compounds,[17]

[†] ETH Zürich.
[‡] University of Bologna.

(1) Quinn, D. M. *Chem. Rev.* **1987**, *87*, 955−979.
(2) Giacobini, E. In *Cholinesterases and Cholinesterase Inhibitors*; Giacobini, E., Ed.; Martin Dunitz Ltd.: London, 2000; pp 181−226.
(3) Soreq, H.; Seidman, S. *Nat. Rev. Neurosci.* **2001**, *2*, 294−302.
(4) Inestrosa, N. C.; Alvarez, A.; Perez, C. A.; Moreno, R. D.; Vicente, M.; Linker, C.; Casanueva, O. I.; Soto, C.; Garrido, J. *Neuron* **1996**, *16*, 881−891.
(5) Bartolini, M.; Bertucci, C.; Cavrini, V.; Andrisano, V. *Biochem. Pharmacol.* **2003**, *65*, 407−416.
(6) Rees, T.; Hammond, P. I.; Soreq, H.; Younkin, S.; Brimijoin, S. *Neurobiol. Aging* **2003**, *24*, 777−787.
(7) Hardy, J.; Selkoe, D. J. *Science* **2002**, *297*, 353−356.
(8) Johnson, G.; Moore, S. W. *Biochem. Biophys. Res. Commun.* **1999**, *258*, 758−762.
(9) De Ferrari, G. V.; Canales, M. A.; Shin, I.; Weiner, L. M.; Silman, I.; Inestrosa, N. C. *Biochemistry* **2001**, *40*, 10447−10457.
(10) Piazzi, L.; Rampa, A.; Bisi, A.; Gobbi, S.; Belluti, F.; Cavalli, A.; Bartolini, M.; Andrisano, V.; Valenti, P.; Recanatini, M. *J. Med. Chem.* **2003**, *46*, 2279−2282.
(11) Recanatini, M.; Valenti, P. *Curr. Pharm. Des.* **2004**, *10*, 3157−3166.
(12) Taylor, P.; Lappi, S. *Biochemistry* **1975**, *14*, 1989−1997.
(13) Nolte, H. J.; Rosenberry, T. L.; Neumann, E. *Biochemistry* **1980**, *19*, 3705−3711.
(14) Ripoll, D. R.; Faerman, C. H.; Axelsen, P. H.; Silman, I.; Sussman, J. L. *Proc. Natl. Acad. Sci. U.S.A.* **1993**, *90*, 5128−5132.
(15) Ordentlich, A.; Barak, D.; Kronman, C.; Flashner, Y.; Leitner, M.; Segall, Y.; Ariel, N.; Cohen, S.; Velan, B.; Shafferman, A. *J. Biol. Chem.* **1993**, *268*, 17083−17095.
(16) Bourne, Y.; Taylor, P.; Radic, Z.; Marchot, P. *EMBO J.* **2003**, *22*, 1−12.
(17) Greenblatt, H. M.; Dvir, H.; Silman, I.; Sussman, J. L. *J. Mol. Neurosci.* **2003**, *20*, 369−384.

10.1021/ja0512780 CCC: $30.25

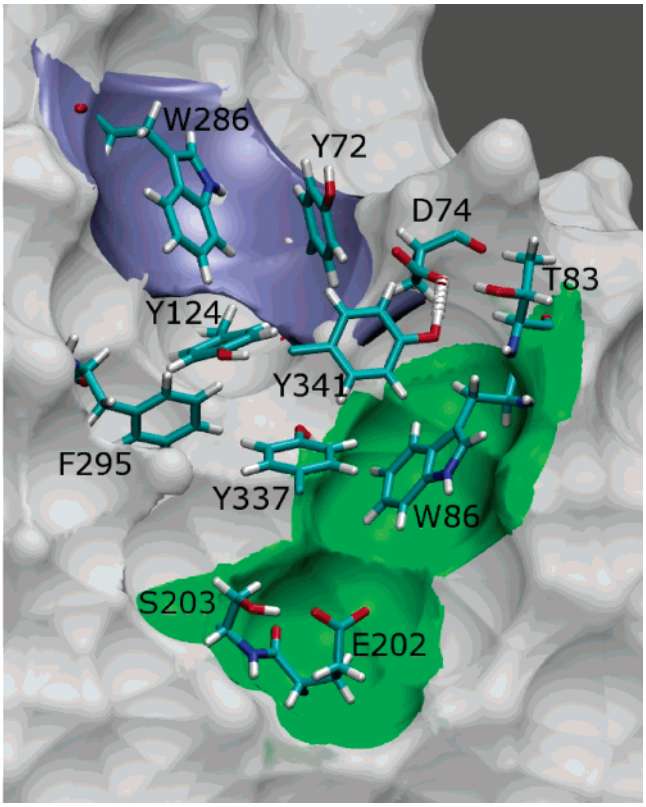

Figure 1. A section of the hAChE gorge. The residues most relevant to the TMA penetration are represented as licorice. The PAS region is highlighted in mauve. The internal part of the gorge and the catalytic site are highlighted in green. The figure was drawn using a relaxed conformation of hAChE taken from the simulation.

allowed the study of AChE−ligand (substrate or inhibitors) interaction mechanism through a multitude of computational methods. The approaches so far followed range from Brownian dynamics/Poisson−Boltzmann[18,19] to Smoluchowski equation,[20] as well as classical molecular dynamics (MD) simulations.[21−26] All the above studies have greatly contributed to the understanding of the enzyme mechanism of action and inhibition. They have shown the role of negatively charged residues on the external surface of the enzyme in capturing the positively charged substrate and funneling it toward the catalytic site.[18,19] Recently, computational studies have been carried out on the PAS and the intermediate layer (16−22 Å from the catalytic site) as well as on the penetration of the ligand in the catalytic pocket of the enzyme. In particular, our group carried out a combined docking/MD simulation study aimed at investigating the binding mode of a cationic selective PAS binder (propidium) of the human AChE (hAChE) PAS.[27] This study allowed us to identify the key interactions between propidium and some PAS residues. In particular, the $\pi-\pi$ stacking between the phenantridinium moiety of propidium and the indole ring of W286 was shown to be the driving force for the binding. Regarding the substrate penetration of the AChE gorge, an MD/umbrella sampling study recently carried out by McCammon and coworkers shed light on the entrance of the tetramethylammonium (TMA) cation into the catalytic region of the murine enzyme (mAChE).[28] According to this study, the rate-limiting step of the entrance is the crossing of a narrow and crowded part of the enzyme gorge from the PAS to the internal anionic site. In particular, a low free energy barrier was found about 12 Å from the catalytic site in good agreement with previously reported experiments.[1] It was, therefore, proposed that the formation/disruption of hydrogen bonds between D74 and Y341 and between D74 and Y124 plays a key role in allowing the ligand to access to the esteratic site. Moreover, a correlation between fluctuations of the diameter of the gorge and the entrance of TMA was identified.[28]

In the present study, both aspects of the ligand penetration, namely, the interaction with the PAS and the penetration in the catalytic pocket, have been considered, and a novel strong relation between the two was found. Using the metadynamics method, which is able to overcome energy barriers and reconstruct free energy surface (FES),[29,30] we investigated the dynamics of the whole process of TMA penetration of the hAChE gorge, with particular respect to the role of both the PAS residues and the cation$-\pi$ interactions in lowering the free energy of the process. By means of metadynamics, many successful penetration events were obtained, and their FES was reconstructed as a function of several sets of collective variables. Our simulations showed that TMA interacts with many aromatic residues of both the surface and the gorge of hAChE by means of cation$-\pi$ interactions, which reveal themselves to be fundamental in the process of TMA penetration. In particular, interactions with the protein electric field and with W286 by means of cation$-\pi$ drove the probe toward the PAS. To further assess the fundamental thermodynamic role of this residue in entrapping TMA at hAChE PAS, the TMA entrance was simulated by employing a single point mutated W286A hAChE. The increased energy barriers revealed by the simulation with the mutant clearly demonstrated the unique role of W286 in driving the ligand recognition and entrance. The main and novel finding of this study is the realization that once the TMA is in the PAS the penetration of the ligand is possible in the presence of a precise and synchronized cascade of events; namely, two cation$-\pi$ interactions are formed and an H-bond is broken. Moreover, we show that the breaking of the H-bond is driven by the presence of the ligand in the PAS.

Methods

General Methods. All simulations were performed using the molecular dynamics program, ORAC,[31] and the AMBER force field.[32] The initial geometry is the same as that used in ref 27 and was obtained

(18) Radic, Z.; Kirchhoff, P. D.; Quinn, D. M.; McCammon, J. A.; Taylor, P. *J. Biol. Chem.* **1997**, *272*, 23265−23277.
(19) Tara, S.; Elcock, A. H.; Kirchhoff, P. D.; Briggs, J. M.; Radic, Z.; Taylor, P.; McCammon, J. A. *Biopolymers* **1998**, *46*, 465−474.
(20) Zhang, D.; Suen, J.; Zhang, Y.; Song, Y.; Radic, Z.; Taylor, P.; Holst, M.; Bajaj, C.; Baker, N. A.; McCammon, J. A. *Biophys. J.* **2004**.
(21) Gilson, M. K.; Straatsma, T. P.; McCammon, J. A.; Ripoll, D. R.; Faerman, C. H.; Axelsen, P. H.; Silman, I.; Sussman, J. L. *Science* **1994**, *263*, 1276−1278.
(22) Tara, S.; Straatsma, T. P.; McCammon, J. A. *Biopolymers* **1999**, *50*, 35−43.
(23) Tara, S.; Helms, V.; Straatsma, T. P.; McCammon, J. A. *Biopolymers* **1999**, *50*, 347−359.
(24) Tai, K.; Shen, T.; Borjesson, U.; Philippopoulos, M.; McCammon, J. A. *Biophys. J.* **2001**, *81*, 715−724.
(25) Tai, K.; Shen, T.; Henchman, R. H.; Bourne, Y.; Marchot, P.; McCammon, J. A. *J. Am. Chem. Soc.* **2002**, *124*, 6153−6161.
(26) Shen, T.; Tai, K.; Henchman, R. H.; McCammon, J. A. *Acc. Chem. Res.* **2002**, *35*, 332−340.
(27) Cavalli, A.; Bottegoni, G.; Raco, C.; De Vivo, M.; Recanatini, M. *J. Med. Chem.* **2004**, *47*, 3991−3999.
(28) Bui, J. M.; Henchman, R. H.; McCammon, J. A. *Biophys. J.* **2003**, *85*, 2267−2272.
(29) Laio, A.; Parrinello, M. *Proc. Natl. Acad. Sci. U.S.A.* **2002**, *99*, 12562−12566.
(30) Iannuzzi, M.; Laio, A.; Parrinello, M. *Phys. Rev. Lett.* **2003**, *90*, 238302.
(31) Procacci, P.; Darden, T. A.; Paci, E.; Marchi, M. *J. Comput. Chem.* **1997**, *18*, 1848−1862.

from the crystal structure of hAChE refined at 2.76 Å resolution in complex with fasciculin (PDB code: 1B41)[33] by removing fasciculin and reconstructing the truncated (268, 291, 369, and 522) as well as the missing (259−264 and 493−494) residues by means of the biopolymer module of the SYBYL 6.8 package (Tripos Inc. St. Louis, MO). The net charge of the enzyme was neutralized by adding seven Na^+ counterions located using the GRID software.[34] The complex was solvated with 14 696 TIP3P water molecules[35] and then relaxed following an annealing scheme, keeping the crystallographic atomic positions fixed. The NPT ensemble was simulated with the Parrinello−Rahman barostat[36,37] and the Nosè−Hoover thermostat,[38] keeping pressure and temperature at 1 atm and 300 K, respectively. A further thermalization run was performed in the canonical ensemble for 0.6 ns at 300 K. In the thermalized structure, the Cα atoms showed an RMSD of 0.98 Å from the crystallographic structure (in Figure 1SI, we reported the RMSD as a function of time of all the atoms of the gorge residues). The parametrization chosen for the TMA was the same as that of Bui et al.,[28] where OPLS charges, nonbonded parameters, and scaling factors[39,40] were used, while keeping AMBER torsional rules.[32] As a test for this parametrization, we calculated the binding energy of TMA to benzene (5.25 kcal/mol), which was slightly better than original AMBER parametrization and in good agreement with ab initio calculations.[41]

The electrostatic potential was calculated by means of the Adaptive Poisson Boltzmann Solver (APBS)[42] with AMBER charges, van der Waals radii, and standard configuration files generated by PDB 2PQR web portal.[43]

To calculate the accessible volume of the hAChE gorge, we defined a cylindrical region of the channel as follows: the axis was defined as the line connecting the S204:Oγ to the geometric center of Cα of residues F295, Y77, and Y72, the height and the radius were chosen to be 23 and 8.5 Å, respectively. This choice ensures that the whole gorge is included. We divided the volume using a grid of 70 × 70 × 70. Each volume element was considered accessible if it was more than a van der Waals radius far from each atom of the enzyme. The total internal accessible area was obtained as a sum of the accessible volume elements. Figures 1 and 7 were realized using the program VMD.[44]

Metadynamics. The metadynamics method[29] was used throughout to accelerate rare events and to reconstruct FESs. In brief, the method is based on a coarse-grained history-dependent potential approach in extended lagrangian framework[30] and relies upon the choice of a set of collective variables (CVs) that can be any function of the atomic positions. Then, an extended lagrangian MD is run, where an additional variable for each CV is added. The additional variables feel the effect of the previous history of the run by means of a Gaussian repulsive potential. This method is able to speed up activated reactions, and if some prerequisites are matched, it is able to reconstruct FESs as functions of the chosen variables within a known and controlled error.[45] The most important requisites are: (i) the reaction coordinate should be mainly a combination of the chosen CVs; (ii) the CVs must be capable of discerning between the initial and final states of the reaction; and (iii) all of the reaction modes having a characteristic time similar to that of the CVs have to be included. For a more detailed description of metadynamics, the interested reader should refer to refs 29, 30, and 46.

In this article, we used metadynamics to study the dynamical motion of a ligand (TMA) from the bulk of the solvent into a 20 Å deep narrow gorge of its biological counterpart (AChE). To this aim, different sets of CVs were employed. The first attempt was made performing a metadynamics with a single CV, the distance between the geometric center of the protein (GEO) and TMA nitrogen atom (namely, TMA:N−GEO distance as a CV). This choice was inspired by the article of Bui et al., who performed an umbrella sampling employing a similar variable.[28] The metadynamics run successfully sampled the TMA entrance, however, requiring other slow degrees of freedom to reconstruct a correct free energy profile. Among these variables, the breaking of an H-bond and the reorientation of aromatic residues were of fundamental importance. Since all preliminary runs, carried out using as a CV only the TMA:N−GEO distance, showed the fundamental role of the cation−π interaction in leading TMA into the hAChE gorge, a new metacoordinate (the cation−π metacoordinate; see below) was developed.

The cation−π metacoordinate was used to monitor both the cation−π interaction with W286 and the sum of n cation−π interactions with inner W86 and F295. Eventually, the CVs used in the present work were the TMA:N−GEO distance and the sum of the cation−π interaction of TMA with W86 and F295; the TMA:N−GEO distance and the cation−π interaction with W286; the TMA:N−GEO distance and TMA:N−W286:Cϵ distance; the TMA:N−GEO distance and TMA:N−A286:Cβ distance in the W286A mutant; D74:Cγ−Y341Oη distance. The following metadynamics parameters were employed. The height of the Gaussians was set to 0.2 kJ/mol and the addition frequency to 300 fs. The width, the coupling constant, and the mass were set to 0.5 Å, 800 kJ/Å^2, 100 amu and 0.12, 8000 kJ/Å^2, 9 amu for the distance and π−cation, respectively. To obtain the optimal FES reconstruction, a metadynamics run should be terminated at the right time. In the present article, the criterion adopted by Gervasio et al.[46] was used. The expected error, calculated according to the formula of Laio et al.[45] is around 0.5 kcal/mol.

The Cation−π Metacoordinate. As discussed above, a new metacoordinate, inspired by the work of Dougherty and Mecozzi,[47,48] was developed. The new metacoordinate describes the cation−π interaction and has the angular dependence of the charge−quadrupole interaction and the slow decay characteristic of cation−π interactions.[47] It is defined as follows:

$$s(\vec{r}_{\mathrm{TMA}},\vec{r}_{1,\mathrm{Aromatic}},\vec{r}_{2,\mathrm{Aromatic}},\ldots)=\sum_{i=1}^{n} f_\theta(\theta_i)\times f_r(\vec{r}_{\mathrm{TMA}}-\vec{r}_{i,\mathrm{Aromatic}})$$

where $\vec{r}_{\mathrm{TMA}}$ is the position of TMA nitrogen, $\vec{r}_{i,\mathrm{Aromatic}}$ is the geometrical center of the ith ring, and θ_i is the angle between the normal to the plane of the ith ring and the distance vector $\vec{r}_{\mathrm{TMA}}-\vec{r}_{i,\mathrm{Aromatic}}$. The two Fermi functions, f_r and f_θ, are defined as follows:

(32) Cornell, W. D.; Cieplak, P.; Bayly, C. I.; Gould, I. R.; Merz, K. M.; Ferguson, D. M.; Spellmeyer, D. C.; Fox, T.; Caldwell, J. W.; Kollman, P. A. *J. Am. Chem. Soc.* **1995**, *117*, 5179−5197.
(33) Kryger, G.; Harel, M.; Giles, K.; Toker, L.; Velan, B.; Lazar, A.; Kronman, C.; Barak, D.; Ariel, N.; Shafferman, A.; Silman, I.; Sussman, J. L. *Acta Crystallogr. D: Biol. Crystallogr.* **2000**, *56*, 1385−1394.
(34) Goodford, P. J. *J. Med. Chem.* **1985**, *28*, 849−857.
(35) Jorgensen, W. L.; Chandrasekhar, J.; Madura, J. D.; Impey, R. W.; Klein, M. L. *J. Chem. Phys.* **1983**, *79*, 926−935.
(36) Parrinello, M.; Rahman, A. *Phys. Rev. Lett.* **1980**, *45*, 1196−1199.
(37) Parrinello, M.; Rahman, A. *J. Appl. Phys.* **1981**, *52*, 7182−7190.
(38) Nosè, S. *Mol. Phys.* **1984**, *52*, 255−268.
(39) Jorgensen, W. L.; Tirado-Rives J. *J. Am. Chem. Soc.* **1988**, *110*, 1657−1666.
(40) Jorgensen, W. L.; Severance, D. L. *J. Am. Chem. Soc.* **1990**, *112*, 4768−4774.
(41) Felder, C.; Jiang, H.; Zhu, W.; Chen, K.; Silman, I.; Botti, S. A.; Sussman, J. L. *J. Phys. Chem. A* **2001**, *105*, 1326−1333.
(42) Baker, N. A.; Sept, D.; Simpson, J.; Holst, M. J.; McCammon, J. A. *Proc. Natl. Acad. Sci. U.S.A.* **2001**, *98*, 10037−10041.
(43) Dolinsky, T. J.; Nielsen, J. E.; McCammon, J. A.; Baker, N. A. *Nucleic Acids Res.* **2004**, *32*, W665−W667.
(44) Humphrey, W.; Dalke, A.; Schulten, K. *J. Mol. Graphics* **1996**, *14*, 33−38.
(45) Laio, A.; Gervasio, F. L.; Fortea-Rodriguez, A.; Ceccarelli, M.; Parrinello, M. *J. Phys. Chem. B* **2005**, *109*, 6714−6721.
(46) Gervasio, F. L.; Laio, A.; Parrinello, M. *J. Am. Chem. Soc.* **2005**, *127*, 2600−2607.
(47) Dougherty, D. A. *Science* **1996**, *271*, 163−168.
(48) Mecozzi, S.; West, A. P., Jr.; Dougherty, D. A. *Proc. Natl. Acad. Sci. U.S.A.* **1996**, *93*, 10566−10571.

$$f(\vec{r}_{\mathrm{TMA}} - \vec{r}_{i,\mathrm{Aromatic}}) = \frac{1}{1 + \exp\dfrac{|\vec{r}_{\mathrm{TMA}} - \vec{r}_{i,\mathrm{Aromatic}}| - \alpha}{\beta}}$$

and

$$f(\theta_i) = \frac{1}{1 + \exp\dfrac{|\theta_i| - \delta}{\gamma}}$$

with $\alpha = 10.0$ Å, $\delta = 0.785$ rad, $\beta = 6.0$ Å, and $\gamma = 0.785$ rad.

θ_i is calculated as

$$\theta_i = \arccos\left(\frac{(\vec{a}_i \times \vec{b}_i)(\vec{r}_{\mathrm{TMA}} - \vec{r}_{i,\mathrm{Aromatic}})}{|\vec{a}_i \times \vec{b}_i||\vec{r}_{\mathrm{TMA}} - \vec{r}_{i,\mathrm{Aromatic}}|}\right)$$

where $\vec{a}_i$ and $\vec{b}_i$ are two vectors which start from the geometric center of the aromatic ring and are pointing to two adjacent carbon atoms of the ith ring. This CV has a strong conical dependence on the angle of approach to the center of the aromatic ring (Figure 2).

Results

TMA Penetration of the hAChE Gorge. The first exploratory metadynamics runs were performed using the TMA:N−GEO distance. An analysis of the run showed that this variable alone was not able to reconstruct the FES since important slow degrees of freedom were not taken into account. Indeed, in the behavior of the metadynamics, the characteristic signatures of a well chosen set of CVs were missing. Namely, at the end of the run, the FES was not flat, resulting in the failure of a diffusive dynamics of the CVs.[45]

However, we obtained several reactive trajectories that were analyzed in order to gain insight on important interactions. The analyses were carried out either by visual inspection of the trajectory or by monitoring several variables. The variables took into account the hydration of the ligand, geometrical parameters related to the opening of the gorge, the orientation of aromatic residues, and the status of several hydrogen bonds. Finally, we singled out a group of variables (Figure 3) that, for all of the analyzed reactive trajectories, correlated to the passage of the TMA from the solution to the internal portion of the gorge, which is defined by a TMA:N−GEO distance of less than 12 Å.

In Figure 3A, the TMA:N−GEO distance of one representative run is reported. First, it shows a failed penetration attempt around 0.5 ns and a successive entrance at 1.5 ns followed at ∼2.4 ns by a re-entry in the solution. By contrasting these two events, we can get an insight into the relevant CVs. We observed that during the failed attempt, the H-bond between the Y341 and D74 (Figure 3B) was formed and only one of the two cation−π interactions between TMA and the aromatic residues W86 and F295 was formed. The successful penetration event required both the breaking of the H-bond and the formation of both cation−π interactions to be favorable. This was further verified by the second part of our metadynamics trajectory. After the re-entry of the TMA in the solution, we would have expected a diffusive behavior of our CV since the energy basins should have been filled, and the resulting FES plus the sum of added Gaussians should have been flat. This did not happen because we did not include in the metadynamics the H-bond and cation−π variables, and they had the wrong value when TMA tried to penetrate in the gorge (see Figure 3 at 3.6 ns, the H-bond is closed and the cation−π is not formed). The trajectory presented in Figure 3 is typical as was verified by several successful penetration events. The last panel in Figure 3 shows that the pure distances between TMA and Cα of both W86 and F295 (Figure 3D) did not show any correlation with either event, underscoring the importance of the orientation of the two aromatic residues. It is to be noted that in their investigation, Bui et al.[28] recognized the importance of the H-bond and imposed it to be open to let the ligand in the gorge.

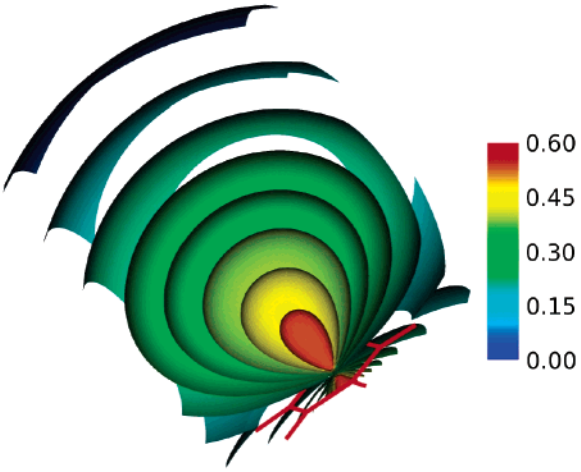

Figure 2. Isosurfaces representing the value of the cation−π order parameter.

Peripheral Anionic Site: The Role of W286. To investigate the role of the hAChE PAS in the TMA recognition and entrance in depth, metadynamics runs were carried out from the external bulk solution to the enzyme PAS. The metadynamics runs were carried out using the TMA:N−GEO distance and the cation−π interaction between TMA and the indole ring of W286 as collective variables. In Figure 4, the FES obtained for the interaction distance between TMA and W286 is reported. In detail, TMA found a well-defined channel, leading it to an external energetic basin (point 1 of Figures 6 and 7), corresponding to the PAS close to the key residue W286. From there, TMA found a relatively low barrier toward the inner part of the hAChE gorge. It was clear that W286 greatly stabilized TMA by means of a cation−π interaction and allowed the ligand to get the proper orientation for a correct gorge entrance.

To further assess the role of W286 for the TMA recognition and orientation, calculations were carried out on a W286A hAChE mutant. Since in W286A mutant, the cation−π interaction was not defined, metadynamics runs were performed using the TMA:N−GEO and the TMA:N−A286:Cβ distances as CVs. Consistently, a successive run was carried out with the wild-type (WT) enzyme using TMA:N−GEO and the TMA:N−W286:Cϵ distances as CVs. In Figure 5, the FESs obtained with the WT (left) and the mutant (right) enzyme are shown. Even at a cursory analysis, it appeared that the FESs were qualitatively different. With the WT enzyme, the FES was very similar to that reported in Figure 4. In contrast, with the W286A mutant, the lack of the PAS key residue W286 caused TMA to spend considerable amount of time close to external residues, such as the negatively charged residues E84 and E91, and the polar ones Q279, Q71, S93, and T75 (data not shown). From Figure 5 (right panel), it can be seen that in the W286A mutant, TMA met higher barriers toward the mouth of the gorge. To further analyze

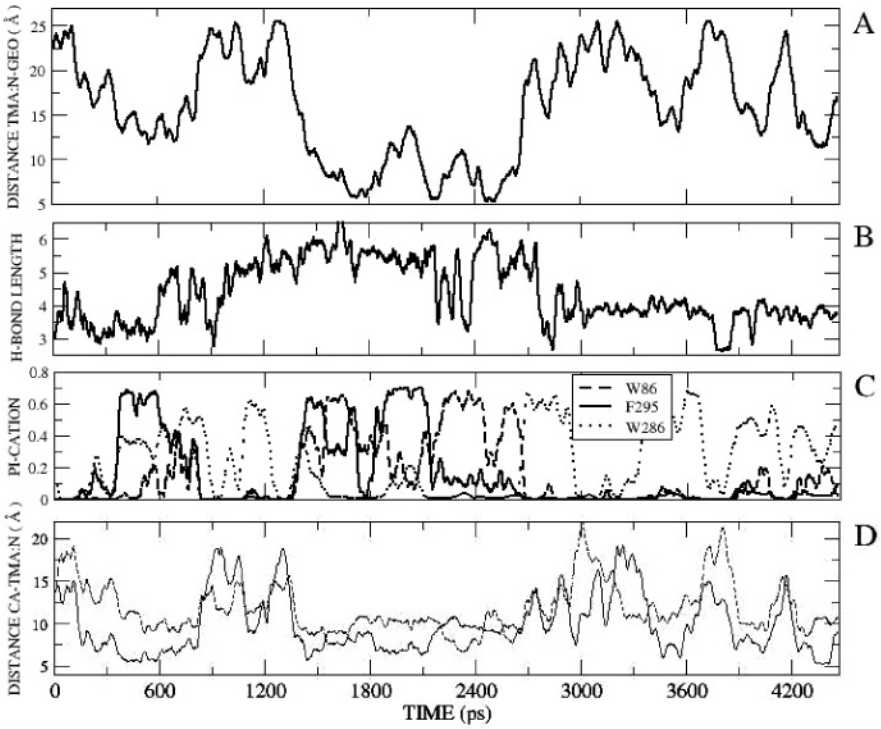

Figure 3. Analysis of a typical reactive trajectory. (A) TMA:N−GEO distance versus the simulation time. The penetration (distance less than 12 Å) seems to be related to the (B) D74−Y341 H-bond breaking (the distance between D74:Cγ−Y341Oη is monitored). (C) The new metacoordinate, *s* (cation−π interaction) between TMA and W86, W286, and F295 is plotted versus the simulation time. When *s* is more than 0.6, the cation−π interaction is formed. (D) Distances between F295:Cα−TMA:N and W86:Cα−TMA:N versus simulation time. Compared to cation−π interactions, such distances are much less efficient in distinguishing between successful and unsuccessful penetration.

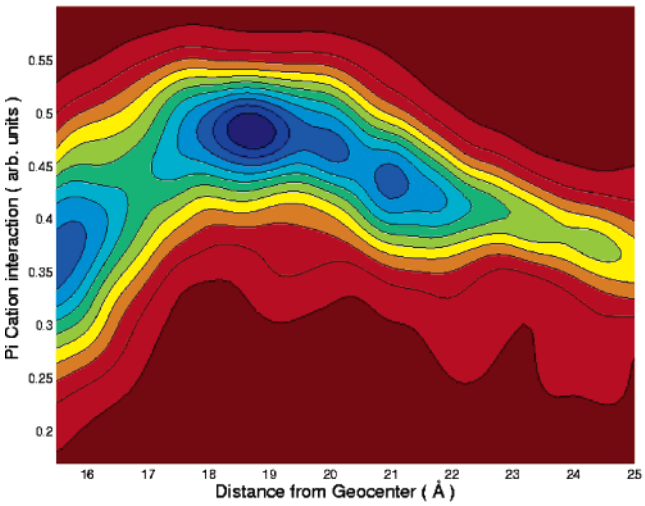

Figure 4. Analysis of bidimensional double collective variables (TMA:N−GEO distance and TMA:N−W286 cation−π interaction) run. Each isosurface is 0.3 kcal/mol, and the colors span from dark red (high energy) to dark blue (low energy).

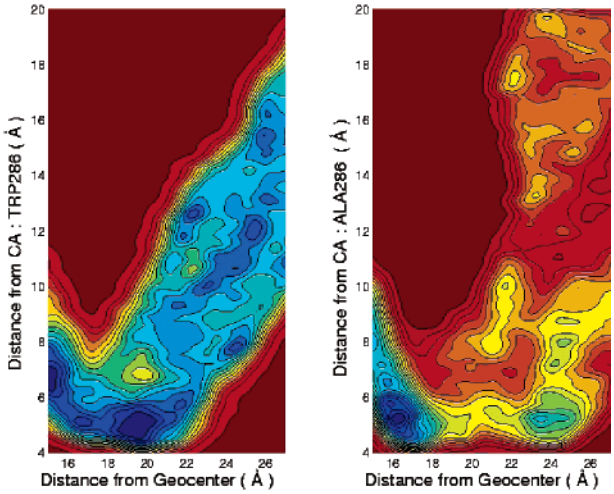

Figure 5. Analysis of bidimensional double collective variables (TMA:N−GEO distance and TMA:N−W(A)286:Cβ distance) run in wild-type (left) and W286A hAChE mutant (right). Each isosurface is 0.3 kcal/mol, and the colors span from dark red (high energy) to dark blue (low energy). It is clear that the lack of van der Waals interactions due to the mutation increases the area spanned by TMA. This greatly reduces the probability of gorge entrance and penetration by increasing the energetic barriers (right).

the nature of this difference, the potential electrostatic maps of the WT and mutant enzyme were generated by means of APBS.[42] It turned out that the potential electrostatic maps were almost identical (data not shown), showing that the charge balance remained almost unaffected by the mutation. The main differences were due to the lack of dispersive (van der Waals) forces, which were not adequately compensated in the W286A mutant by an increase of width of the gorge entrance that could be expected to be somehow responsible for a decrease of entrance barriers.

Reconstruction of the TMA Penetration FES. When most of the information on the main interactions enabling the ligand penetration of the gorge was acquired, the FES of the TMA entrance was studied. After several trials, it was found that the best set of CVs to be used in the free energy estimation was composed by TMA:N−GEO distance along with the cation−π interaction between TMA and both W86 and F295. The FES profile projected on the TMA:N−GEO distance dimension is

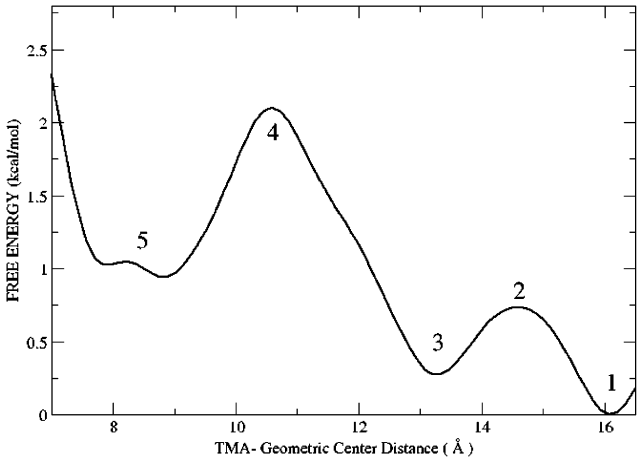

Figure 6. FES of metadynamics runs carried out in the inner part of the gorge employing as CVs TMA:N−GEO distance and the sum of cation−π interactions with W86 and F295. The FES is projected as function of TMA: N−GEO distance.

shown in Figure 6, while in Figure 7, snapshots of metadynamics, corresponding to stationary points 1−5 of Figure 6, are reported.

A movie showing the trajectory schematized in Figure 7 is available as Supporting Information.

The barrier to the entrance was calculated to be 1.8 kcal/mol (7.5 kJ/mol) after 1.6 ns of metadynamics. Three main energetic basins were found (marked as 1, 3, and 5 in Figures 6 and 7). The first basin (1 in Figures 6 and 7) is located at about 16 Å and corresponds to the PAS region. This region was explored in depth while studying the external part of the enzyme (see above). The second basin (3 in Figures 6 and 7) is located at about 13.5 Å and was due to stabilizing interactions with the partially internal residues D74 and Y341. The crossing of the barrier (2 in Figures 6 and 7) between these basins was possible only if a complex series of events took place. In details, the cation−π interaction with F295 increased driving the ligand from the PAS to Y341:O. As the breaking of the D74−Y341 H-bond occurred, the strong interaction with Y341:O was lost (point 2 of Figure 7). The negative charges of D74 as well as the aromatic moiety of W86 led TMA toward a cation−π interaction with Y341 (point 3 of Figure 7). The major effort, namely, the transition state of the TMA penetration, is to cross the plane composed by Y124 and Y337 (point 4 of Figures 6 and 7). This passage is eased by the breaking of the Y341−D74 H-bond that enlarges the gorge (see Figure 7, point 4). This H-bond breaking is energetically compensated by the formation of an Y341−T83 H-bond.

The final position of TMA (point 5 of Figures 6 and 7) is stabilized both by a strong cation−π interaction with W86 and by the negative charge of E202.

Role of the PAS in Breaking the D74−Y341 H-Bond. In our simulations, in agreement with the results of McCammon and co-workers,[28] the breaking of D74−Y341 H-bond turned out to be a fundamental event for the TMA entrance. In particular, the breakage of such an interaction enlarged the mouth width, as shown in Figure 8, exposed W86 for the cation−π interaction with TMA, and allowed a reorientation of Y341 for a proper cation−π interaction with the ligand that lowered the transition state energy of point 2 (Figure 6). To test this hypothesis more in depth, we performed a constrained metadynamics run in which we kept the H-bond "formed" by applying an harmonic potential of 100 kJ mol^{-1} Å^{-2} to the distance between the oxygens of tyrosine and aspartate. As expected, the free energy basin corresponding to the cation−π interaction between TMA and W86 was no longer accessible, and the TMA fluctuated at the enzyme PAS. In Figure 9, the maps corresponding to the entrance of TMA with the H-bond free (left) and constrained in the closed state (right) are reported. Keeping the H-bond free to be formed (closed state) and broken (open state), the TMA entrance was allowed only in the open state. Conversely, the H-bond constrained in the closed state prevented the hAChE gorge crossing by TMA and, eventually, the interaction between TMA and W86 (in Figure 9, see the free energy basin at about 8.5 Å).

A question that remained open was the role of the PAS in the H-bond opening. In Figure 10, the FES of the H-bond Y341−D74 breaking in the presence and in the absence of TMA in the PAS is reported. From the plot, it is evident that the presence of TMA in the PAS had a dramatic effect on the energetic of the H-bond. In the case of the water-solvated TMA-free enzyme, the H-bond was preferentially closed, as expected. We then introduced a TMA in the PAS. Since the PAS is a relatively deep energetic well for the TMA, it remained close to the initial position during the whole simulation. The presence of the TMA in the PAS reversed the energetic of the H-bond, with a clear-cut preference for an open H-bond. This finding shows the importance of the PAS in easing the entrance of the TMA in the gorge.

Discussion and Conclusions

The role of both cation−π interactions and the PAS in the TMA entrance of the hAChE gorge were investigated by means of metadynamics simulations. We showed the suitability of the metadynamics method to study the multidimensional FESs of a ligand (TMA) recognition, entrance, and penetration of its biological counterpart (hAChE), confirming the positive track record obtained by metadynamics in many related problems, spanning from ligand docking[46] to the translocation of an antibiotic through a membrane channel.[49]

By studying the WT and the W286A mutant, we showed that the PAS and its aromatic residue W286 have a unique role in capturing TMA from the solvent and stabilizing it close to the aromatic cage. The diffuse negative π cloud of the indole ring is well suited to interact with quaternary cation.[47,50] As previously suggested for propidium,[27] only interactions such as $\pi-\pi$ stacking or cation−π might be able to catch N-quaternary ligands from the aqueous environment. Indeed, the cationic nature of TMA is responsible for strong interaction with water, and only the AChE electric field[51] together with cation−π interactions with W286 is able to extract these charged ligands from the bulk solution, stabilize, and orient them properly for the gorge entrance.

Starting from the PAS, the whole process of TMA entrance was studied all the way to the internal anionic site. The obtained free energy profile reported in Figure 6 is remarkably similar

(49) Ceccarelli, M.; Danelon, C.; Laio, A.; Parrinello, M. *Biophys. J.* **2004**, *87*, 58−64.
(50) Dougherty, D. A.; Stauffer, D. A. *Science* **1990**, *250*, 1558−1560.
(51) Botti, S. A.; Felder, C. E.; Lifson, S.; Sussman, J. L.; Silman, I. *Biophys. J.* **1999**, *77*, 2430−2450.

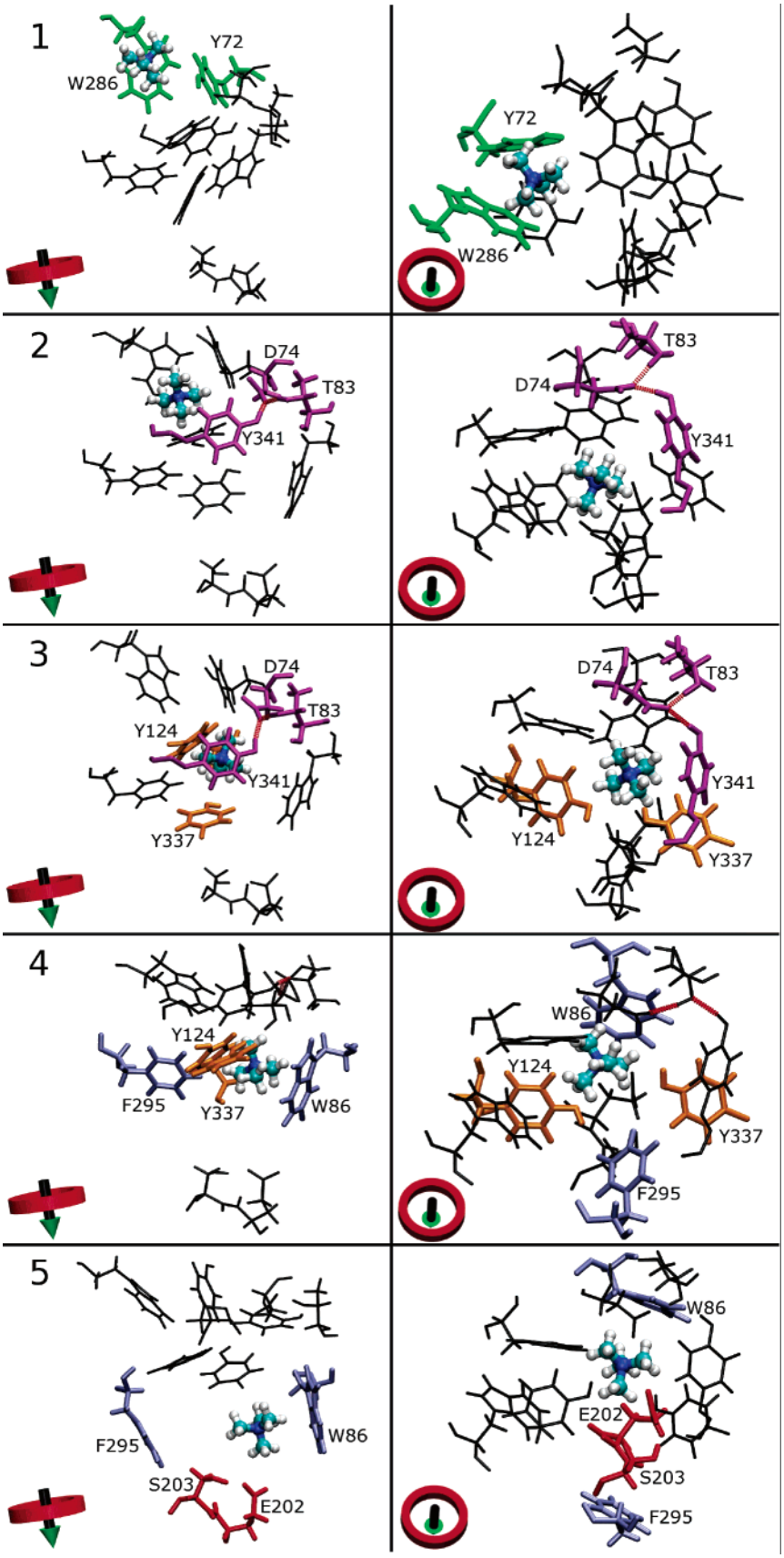

Figure 7. Five snapshots (along the axis of the gorge in the first column and perpendicular to this in the other, see bottom-left indicators) of metadynamics corresponding to points 1−5 of Figure 6. The PAS residues W286 and Y72 are green. In purple, Y341, D74, and T83 are responsible for the forming/breaking of a key H-bond. In orange, are Y124 and Y337 that form the plane which TMA has to pass through (the transition state) to reach the internal anionic site. In blue, W86 and F295 are responsible for key cation−π interactions during TMA motions within the hAChE gorge, and in red, S203 and E202 representing the bottom of the gorge are shown.

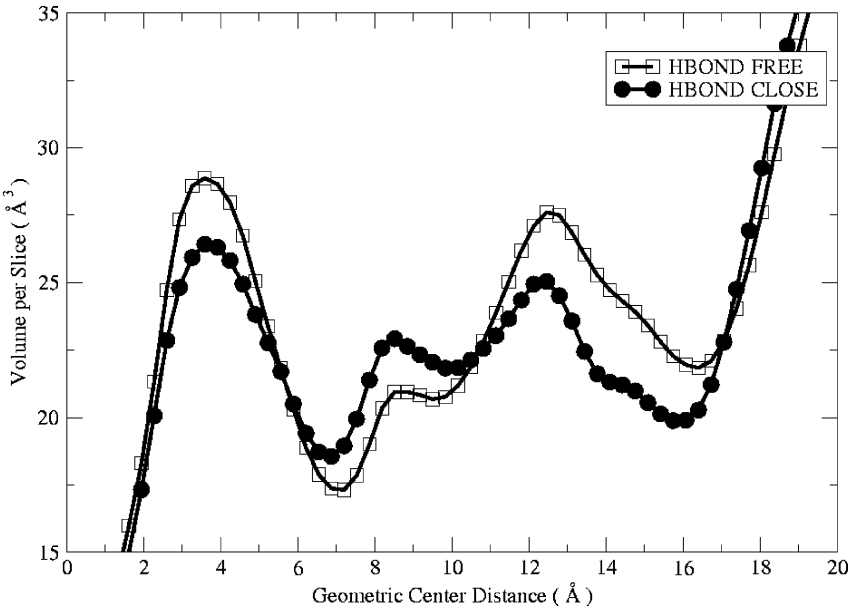

Figure 8. Accessible volume analysis for close H-bond and free H-bond configuration. Each volume slice is 0.32 Å thick.

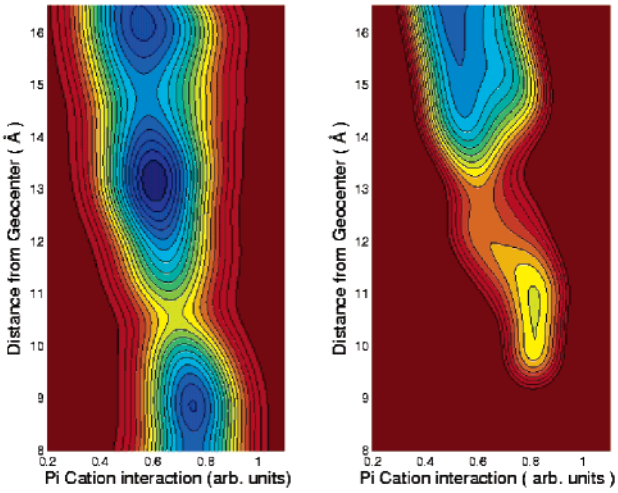

Figure 9. Analysis of bidimensional double collective variables (TMA:N−GEO distance and TMA:N−W286 cation−π interaction) run with free (left) and closed (right) H-bond. Each isosurface is 0.3 kcal/mol, and the colors span from dark red (high energy) to dark blue (low energy).

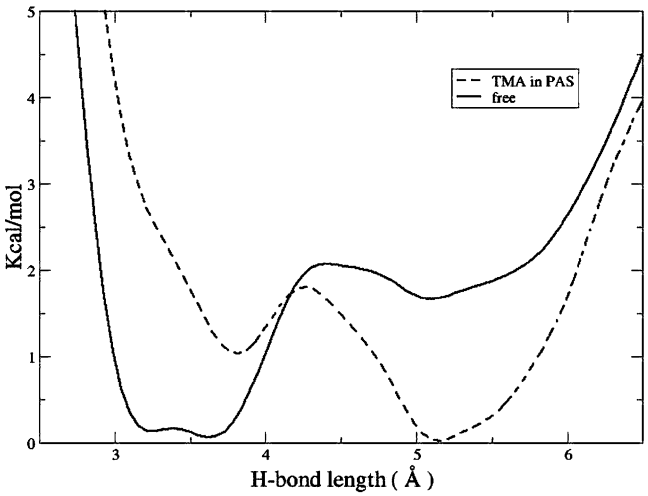

Figure 10. FES of the D74:Cγ−Y341Oη distance, representative of the H-bond between the two residues. The continuous and broken line is the FES obtained with a TMA in the PAS and in absence of TMA, respectively.

to that obtained by McCammon and co-workers, performing an umbrella sampling study on the mAChE.[28] In this respect, the barrier to the entrance (7.5 kJ/mol) is very similar to that reported by these authors (8−10 kJ/mol)[28] and in very good agreement with experiments indicating that AChE operates in the diffusion-controlled limit.[1] A key difference between the umbrella sampling study and our metadynamics simulations resides in the capability of the latter for fast reconstruction of multidimensional FESs.[28] This enabled us, among other things, to obtain a spontaneous opening of the gorge during the run and to point out the importance of cation−π interactions.

Two key events are responsible for the ligand entrance: the D74−Y341 H-bond breaking with the Y341 aromatic plane reorientation, and the synchronous formation of cation−π interactions with both W86 and F295 of the internal anionic site.

The importance of the bond breaking was already pointed out in the study by McCammon and co-workers,[28] but here we show, for the first time, that the residence of TMA in the PAS changes the energetic of the gorge, leading to a spontaneous opening of this H-bond.

Moreover, a central role for the cation−π interaction in the TMA entrance is clearly highlighted, confirming early proposals derived from experimental evidence. Indeed, the role of cation−π interaction in the penetration of quaternary compounds into the AChE gorge has been proposed as early as the first crystal structure from *Torpedo californica* was solved by Sussman et al.[52] Later, Shafferman and co-workers provided direct proof of the fundamental contribution of the cation−π in the interaction between hAChE and N-quaternary ligands.[15] Our finding is further proven by the dramatic decrease of catalytic activity of the W86A mutant, which showed a K_M for N-quaternary ligands as much as 660-fold larger than that of the WT hAChE.[15]

(52) Sussman, J. L.; Harel, M.; Frolow, F.; Oefner, C.; Goldman, A.; Toker, L.; Silman, I. *Science* **1991**, *253*, 872−879.

Acknowledgment. A.C. and M.R. acknowledge support from the University of Bologna (funds for selected research topics). F.L.G. is grateful to L. Gilly for useful discussions.

Supporting Information Available: A movie showing the ligand entrance in the gorge. The ligand from the PAS enters the internal anionic site. A figure showing the RMSD as a function of time for the atoms of the residues in the gorge. This material is available free of charge via the Internet at http://pubs.acs.org.

JA0512780